J Mater Sci (2007) 42:5465–5469
DOI 10.1007/s10853-006-0773-5

Structural and magnetic properties of strontium–borate glasses containing iron ions

I. Ardelean · R. Lungu · P. Păşcuţă

Received: 6 April 2006 / Accepted: 7 August 2006 / Published online: 23 March 2007

Abstract Glasses of the $x Fe_2O_3 \cdot (100 - x)[B_2O_3 \cdot SrO]$ system, with $0 \le x \le 30$ mol%, were studied by EPR and magnetic susceptibility measurements. EPR spectroscopy and magnetic susceptibility measurements show that the Fe^{3+} ions are localized in sites of distorted octahedral symmetry and in clustered formations containing both Fe^{3+} and Fe^{2+} ions. Dipolar and superexchange interactions involving iron ions were revealed depending on the iron content of the sample.

Introduction

The wide variety of properties of glasses led to the wide interest in the investigation of physical and chemical properties of these materials and their composition dependence [1]. Borate glasses are usually characterized by having interesting properties of great value for industrial exploitation [1–3]. These properties are commonly attributed to the fact that the boron atom can assume trigonal and tetrahedral coordinations and also to the different ways through which the borate building units can be linked together [1]. The addition of iron ions to borate glasses makes them superparamagnetic and electrically semiconducting [4, 5]. Iron ions in these glasses are considered to assemble together and form clusters which exhibit superparamagnetic behaviour and below the freezing temperature, individual spins are frozen in random directions because of antiferomagnetic interaction between nearby ions [5]. A general condition for semiconducting behaviour of borate glasses containing iron ions is the coexistence of iron ions in more than one valence state, Fe^{2+} and Fe^{3+} [6], but only Fe^{3+} ($3d^5$, $^6S_{5/2}$) shows EPR absorptions at room temperature [7–9]. EPR of Fe^{3+} ions may provide useful information concerning the structural details of the vitreous matrix revealed by their distribution on different structural units building the network, their coordination and the valence state. It is also possible to follow the structural changes in the matrix when iron ions concentration increases during a controlled doping process.

Magnetic susceptibility measurements revealed as very useful to determine the valence states of transition metal ions and the type of interactions involving them over various composition ranges. Their magnetic properties depend on the concentration of the 3d element and the valence states ratio [10, 11] as well as on the structure of the vitreous matrix and implicitly on the conditions of sample preparation [12]. The superexchange interaction of the iron ions in the oxide glasses was most frequently attributed to an antiferromagnetic coupling within the pairs Fe^{3+}–Fe^{3+}, Fe^{3+}–Fe^{2+} and Fe^{2+}–Fe^{2+} [13, 14]. An antiferromagnetic coupling between iron ions was reported in borate [15, 16], phosphate [13, 17], tellurite [18, 19], bismuthate [20], silicate [21] and germanate [22] oxide glasses.

This work aims to present our results obtained by means of EPR and magnetic susceptibility measurements performed on $B_2O_3 \cdot SrO$ glass matrix gradually doped with Fe_2O_3. The research is part of a comparative analysis program focused on the behaviour of transition metal ions in vitreous oxide matrices.

I. Ardelean (✉) · R. Lungu
Faculty of Physics, Babes-Bolyai University, 400084
Cluj-Napoca, Romania
e-mail: arde@phys.ubbcluj.ro

P. Păşcuţă
Department of Thermothecnics, Techical University, 400641
Cluj-Napoca, Romania

Experimental procedure

The starting materials used in the present investigation were Fe_2O_3, H_3BO_3 and $SrCO_3$ of reagent grade purity. The samples were prepared by weighing suitable proportions of components, powder mixing and mixture melting in sintered corundum crucibles at 1,200 °C for 30 min. The mixtures were put into the furnace direct at this temperature. The melts were poured onto stainless steel plates.

The X-ray diffraction measurements were made with a diffractometer Philips X'Pert MPD, with a monochromator of graphite for CuK_α (λ = 1.540560 Å). The pattern obtained did not reveal any crystalline phase in the samples up to 30 mol% Fe_2O_3. For the sample with x = 40 mol% a crystalline phase of Fe_2O_3 was pointed out near the vitreous phase.

The electron paramagnetic resonance (EPR) measurements were made using a Portable Adani PS 8400 spectrometer in X-band (9.1–9.6 GHz). The measurements were made at room temperature. To avoid the alteration of the glass structure due to the ambient conditions, especially humidity, samples were poured immediately after preparation and enclosed in tubular holders of the same caliber. Equal quantities of samples were studied.

The magnetic susceptibility measurements were made using a Faraday type magnetic balance in 80–300 K temperature ranges. Correction due to the diamagnetism of the Fe_2O_3, B_2O_3 and SrO were taken into account in order to obtain the real magnetic susceptibility of manganese ions in the studied glasses.

Results

EPR data

For exploring the structure of the studied glasses Fe^{3+} ($3d^5$; $^6S_{5/2}$) ions were chosen as paramagnetic probes in EPR measurements. The absorption spectra being sensitive at the symmetry of the structural units which are building up the network and giving information about the involved paramagnetic ions, valence states and interactions. The features of the recorded spectra are detailed in Fig. 1. As can be seen from the Fig. 1, there is a strong dependence of the absorption spectra structure and parameters on the Fe_2O_3 content of the samples. The resonance spectra mainly consist in absorption lines centred at $g_{eff} \approx 4.3$ for samples with $0.5 \le x \le 20$ mol% and $g_{eff} \approx 2.0$ for all investigated concentration range, respectively. The evolution of the resonance lines with increasing of iron ions content was followed in the dependence of the EPR parameters, i.e., the line intensity J, estimated as the line integral and the peak-to-peak line width ΔB. The corresponding variations of these parameters are plotted in Figs. 2, 3 for the resonance lines at $g_{eff} \approx 4.3$ and $g_{eff} \approx 2.0$, respectively.

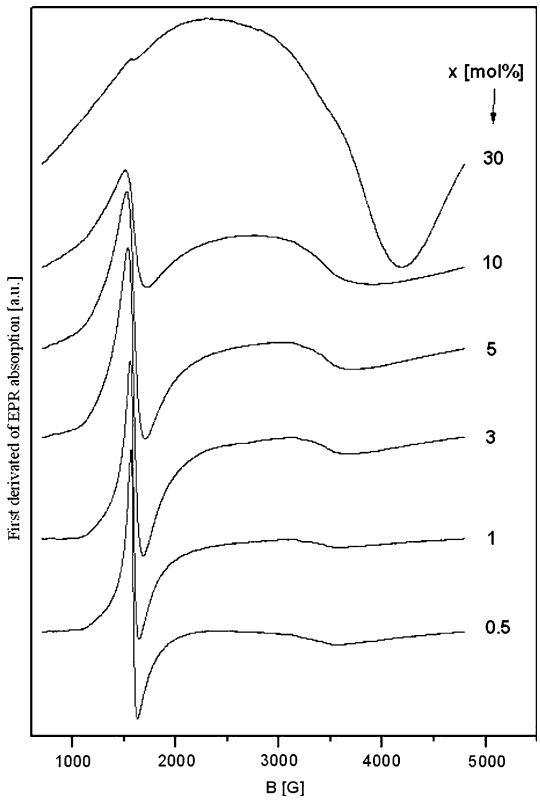

Fig. 1 EPR absorption spectra of Fe^{3+} ions in $x$$Fe_2O_3$·(100 – x) [B_2O_3·SrO]glasses

Magnetic susceptibility data

The temperature dependence of the reciprocal magnetic susceptibility of some glasses from the investigated system is presented in Fig. 4. The concentration dependence of the paramagnetic Curie temperature (θ_p) is given in Fig. 5. The molar Curie constant values, C_M, are given in Table 1.

Discussion

EPR spectra typical for Fe^{3+} ($3d^5$; $^6S_{5/2}$) paramagnetic ions were obtained (Fig. 1). They attest the presence of the iron ions in the (3+) valence state for all the investigation samples. The resonance spectra mainly consist in absorption lines centred at $g_{eff} \approx 4.3$ for samples with $0.5 \le x \le 20$ mol% and $g_{eff} \approx 2.0$ for all investigated concentration range, respectively. Their prevalence in the spectrum depends on the Fe_2O_3 content of the samples (Fig. 1). The EPR parameters of the absorption lines also depend on iron concentration (Figs. 2, 3).

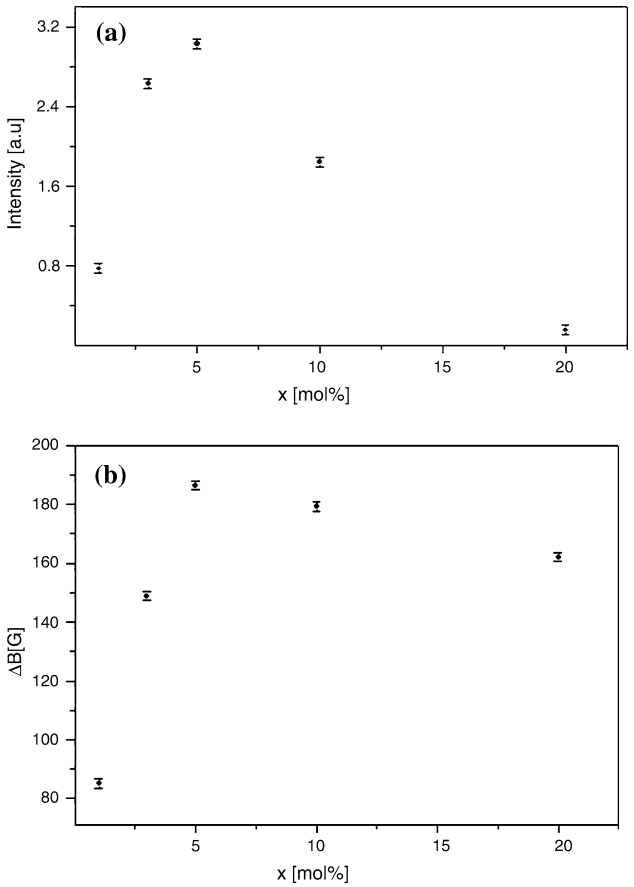

Fig. 2 Composition dependences of the line intensity (**a**) and line width (**b**) of resonance absorptions at $g_{\text{eff}} \approx 4.3$

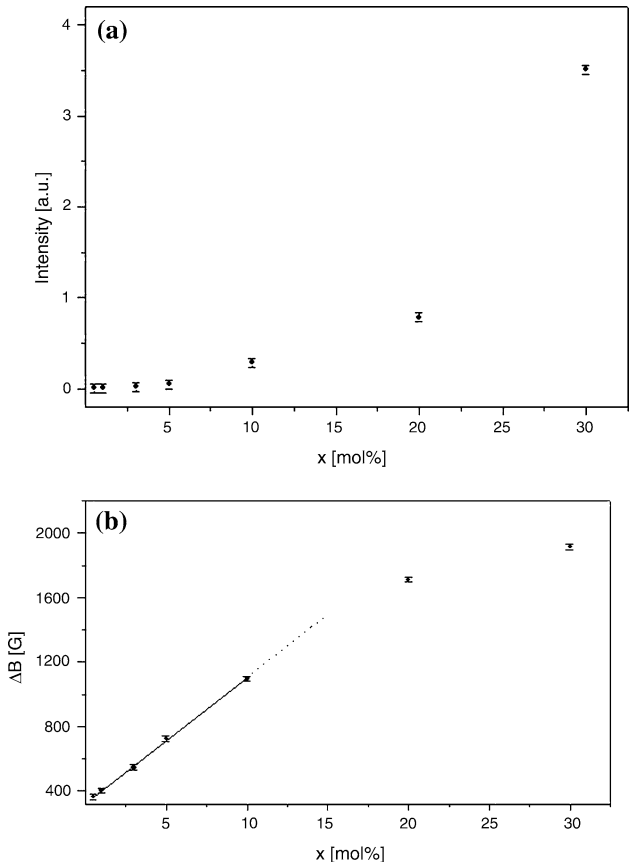

Fig. 3 Composition dependences of the line intensity (**a**) and line width (**b**) of resonance absorptions at $g_{\text{eff}} \approx 2.0$

The resonance line at $g_{\text{eff}} \approx 4.3$ is due to Fe^{3+} ions which are isolated and situated in sites of distorted octahedral symmetry (rhombic or tetragonal) subjected to strong crystal field effects [8, 23–25]. The absorption may induce transitions between the medians Kramers doublet lines when the site symmetry is rhombic [23, 24, 26] or between the lines of the lowest doublet, in the case of tetragonally [8] or cubic tetragonally distorted sites [27]. The intensity of this resonance absorption line increases until $x = 5$ mol% then it decreases at higher content of Fe_2O_3 (Fig. 2a). The decreasing of this resonance line intensity at the same time with the increasing of the Fe_2O_3 content is due to the destruction of the configuration from the iron ions neighbourhood, which assures their magnetic isolation. The structural units of defined symmetry involving Fe^{3+} ions although randomly distorted, have at the origin the structure of glass matrix former, B_2O_3. These structural units assure the independence of the involved Fe^{3+} ions and their specific state of energy. The gradual increasing of the iron content in the matrix destroys the local ordering of the Fe^{3+} ion neighbourhood, so the structural units as characteristic entities become less represented. Consequently the $g_{\text{eff}} \approx 4.3$ line intensity decreases. The line width evolution of the $g_{\text{eff}} \approx 4.3$ resonance absorption (Fig. 2b) shows an increasing up to $x = 5$ mol%. For higher content of Fe_2O_3, the line width decreases. According to the line intensity decreasing evidenced for $x > 5$ mol% (Fig. 2a), the decreasing of ΔB is due to the progressive decrease of the concentration of Fe^{3+} ions in structural vicinities giving rise to the $g_{\text{eff}} \approx 4.3$ absorption.

The $g_{\text{eff}} \approx 2.0$ line may be attributed either to Fe^{3+} species interacting by dipole–dipole interaction in sites of less distorted octahedral (tetrahedral) field and/or to superexchange coupled pairs [9, 28]. The composition dependence of this absorption line intensity shows an increasing in all whole concentration range, more evidenced for $x > 5$ mol% (Fig. 3a). On the other hand, the line intensity of the absorptions at $g_{\text{eff}} \approx 4.3$ decreases for $x > 5$ mol% (Fig. 2a), in consequence, at higher content of Fe_2O_3 ($x > 5$ mol%), the Fe^{3+} ions participated at dipole–dipole and/or superexchange interactions. The line width of the $g_{\text{eff}} \approx 2.0$ resonance absorption depends also on the

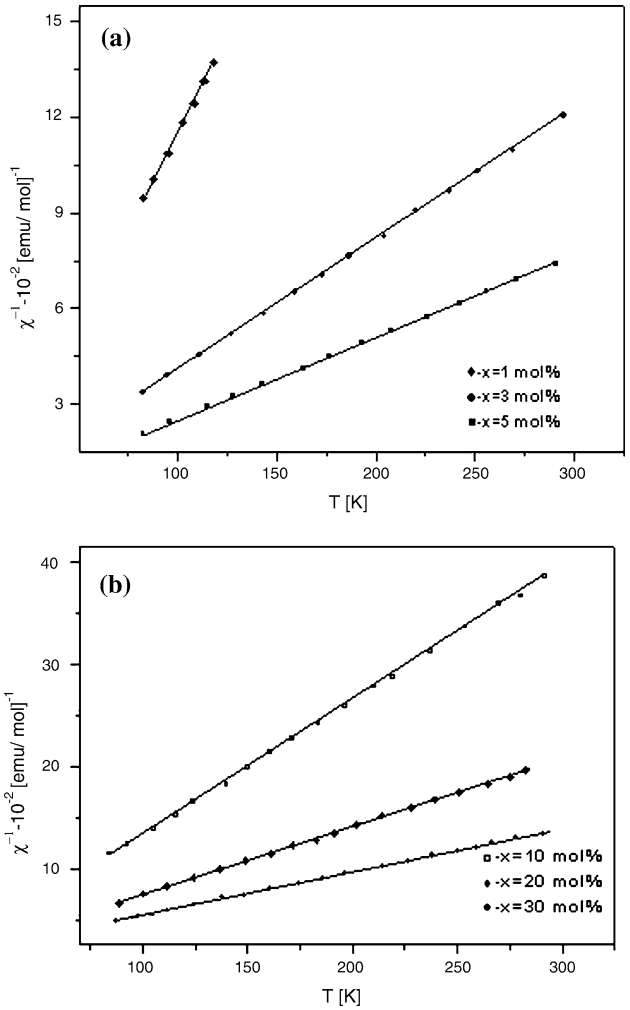

Fig. 4 Temperature dependence of the reciprocal magnetic susceptibility for $x\mathrm{Fe_2O_3}\cdot(100-x)$ $[\mathrm{B_2O_3}\cdot\mathrm{SrO}]$ glasses with $1 \le x \le 5$ mol% (**a**) and with $10 \le x \le 30$ mol% (**b**)

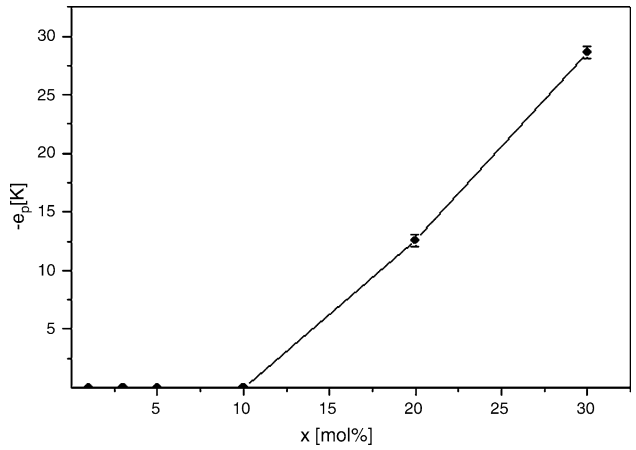

Fig. 5 Composition dependence of the paramagnetic Curie temperature

Table 1 Molar Curie constant, molar fraction of $Fe^{3+}(x_1)$ and $Fe^{2+}(x_2)$ ions in $x\mathrm{Fe_2O_3}\cdot(100-x)$ $[\mathrm{B_2O_3}\cdot\mathrm{SrO}]$ glasses

x (mol % Fe_2O_3)	$C_M \pm 1\cdot10^{-4}$ (emu/mol)	x_1 (mol% $Fe_2^{3+}O_3$)	x_2 (mol% $Fe_2^{2+}O_3$)
1	0.0845	0.9	0.1
3	0.2455	2.3	0.7
5	0.3920	3.3	1.7
10	0.7589	5.7	4.3
20	1.5085	10.9	9.1
30	2.3696	20.3	9.7

Fe_2O_3 concentration (Fig. 3b) revealing the clustering capacity of the iron ions in the investigated matrix. The $\Delta B = f(x)$ dependence reflects the competition between the broadening mechanisms as the dipol–dipol interactions, the increased disordering of the matrix structure, the interactions between ions in multivalent states and the narrowing ones that are the superexchange interactions within the pairs of iron ions. These mechanisms can act simultaneously but they are predominant in function of the Fe_2O_3 sample content. Following the $\Delta B = f(x)$ dependence it was observed a deviation from linearity of ΔB at $x > 10$ mol%. This suggests that for $x > 10$ mol% can appear superexchange interactions between iron ions which narrow the resonance line from $g \approx 2.0$.

The magnetic susceptibility data correlate well with the EPR result and also complete them. The temperature dependence of the reciprocal magnetic susceptibility is given in Fig. 4. For glasses containing $x \le 10$ mol% the Curie law is obeyed, suggesting existence of isolated iron ions or/and subjected to dipole–dipole interactions. For $x > 10$ mol% the reciprocal magnetic susceptibility obeys a Curie–Weiss law with negative paramagnetic Curie temperature characteristic to antiferromagnetic coupling of magnetic ions. The peculiar structure specific to vitreous oxide glasses impose the short-range character of magnetic interactions and enhance the structural image of clusters. The result agrees with data explaining the $g \approx 2.0$ lines narrowing as result of superexchange interactions between iron ions involved in cluster structure. The composition dependence of θ_p is given in Fig. 5. The absolute value of θ_p increases for $x > 10$ mol% with the magnetic ions content of the sample. The composition dependence of the molar Curie constant (C_M) is presented in Table 1. For all the glasses experimental values obtained for molar Curie constant and consequently for effective magnetic moments are lower than those which correspond to the Fe_2O_3 content, considering that all iron ions are in Fe^{3+} valence state, but they are higher than those calculated for the case when all iron ions would be Fe^{2+} species (Table 1). Therefore we

consider that in these glasses are present both Fe^{3+} and Fe^{2+} ions. The presence of Fe^{3+} and Fe^{2+} ions has been evidenced in other oxide glasses [11, 12, 16–20]. Having in view this supposition and using the atomic magnetic moment values of free Fe^{3+} and Fe^{2+} ions: $\mu_{Fe}^{3+}=5.92\mu_B$ and $\mu_{Fe}^{2+}=4.90\mu_B$ [29], we can estimate in first approximation the molar fraction of these ions in the investigated glasses using the relations:

$$x \cdot \mu_{eff}^2 = x_1 \cdot \mu_{Fe^{3+}}^2 + x_2 \cdot \mu_{Fe^{2+}}^2$$

and

$$x = x_1 + x_2,$$

where $\mu_{eff} = 2.827 \cdot [C_M/2x]^{1/2}$ are the experimental magnetic moment, x_1 and x_2 are the molar fraction of iron ions in $Fe^{3+}$and Fe^{2+} valence states. The results are presented in Table 1. From these data one remarks that the molar fraction of both Fe^{3+} and Fe^{2+} ions increases in whole studied concentration range, the proportion of Fe^{3+} ions being prevalent.

Conclusions

Glasses of the system $xFe_2O_3 \cdot (100 - x)[B_2O_3 \cdot SrO]$ were obtained over the $0 \le x \le 30$ mol% concentration range.

EPR absorption spectra due to Fe^{3+} ions were detected within $0.5 \le x \le 30$ mol%. The structure of the spectra and the values of the EPR parameters of resonance lines depend on the Fe_2O_3 concentration. The isolated Fe^{3+} ions in sites of distorted octahedral symmetry subjected to strong crystalline field effects were detected over a relatively broad concentration range, attesting the structural ability of the vitreous matrix in receiving these ions.

The EPR and magnetic measurements revealed both dipolar and superexchange-type interactions involving iron ions. For samples with $x > 10$ mol% antiferromagnetically coupled iron ions were evidenced.

References

1. Abo-Naf S, Darwish H, El-Desoky MM (2002) J Mater Sci Mater Electron 13:537
2. Mazelev YA (1960) Borate glasses. Consultants Bureau, New York
3. Volf MB (1990) Technical approach to glass. Elsevier, Amsterdam
4. Collins DW, Mulay LN (1971) J Am Ceram Soc 54:69
5. El-Desoky MM, Abo-Naf S (2004) J Mater Sci Mater Electron 15:425
6. Murawski L, Barczynski RJ (1995) J Non-Cryst Solids 185:84
7. Murawski L, Chung CH, Mackenzie JD (1979) J Non-Cryst Solids 32:91
8. Cerny V, Petrova B, Fumar M (1990) J Non-Cryst Solids 125:17
9. Ardelean I, Peteanu M, Filip S, Simon V, Gyroffy G (1997) Solid State Commun 102:341
10. Wickman HH, Klein MP, Shirlei DA (1965) J Chem Phys 42:2113
11. Ardelean I, Pascuta P, Ioncu V (2001) Mod Phys Lett B 15(30):1445
12. Ardelean I, Peteanu M, Simon V, Filip S, Ciorcas F, Todor I (1999) J Magn Magn Mater 197:258
13. Wilson LK, Friebele EJ, Kinser DL (1975) In: Proceedings of the international symposium on amorphous magnetism. Plenum Press, New York, p. 65
14. Ardelean I, Peteanu M, Filip S, Simon V, Győrffy G (1997) Solid State Commun 102:341
15. Burzo E, Ardelean I (1979) Phys Chem Glasses 20:15
16. Ardelean I, Pascuta P, Peteanu M (2002) Mod Phys Lett B 16(7):231
17. Kumar B, Chen CH (1994) J Appl Phys 75:6760
18. Ardelean I, Hong-Hua Q, Sakata H (1997) Mater Lett 32:335
19. Ardelean I, Satou H, Sakata H (Studia Univ. Babes-Bolyai) (1998) Physica XLIII(2):3
20. Ardelean I, Ilonca Gh, Cozar O, Simon V, Filip S (1994) Mater Lett 21:321
21. Mekki A, Ziq KhA (1998) J Magn Magn Mat 189:207
22. Mekki A, Holland D, Ziq KhA, McConviele CF (2000) J Non-Cryst Solids 272:179
23. Castner T, Newell GS, Holton WC, Slichter CP (1960) J Chem Phys 32:668
24. Loveridge D, Parke S (1971) Phys Chem Glasses 12:19
25. Griscom DL (1980) J Non-Cryst Solids 40:211
26. Kedzie RW, Lyons DH, Kestigian M (1960) Phys Rev 138A:918
27. Cerny JV, Frumarova B, Rosa J, Licholit IL, Urban P (1974) Phys Stat Sol (b) 61:475
28. Chaudhuri SP, Patra SK (2000) J Mat Sci 35:4735
29. Mulay LM (1973) Magnetic susceptibility. Interscience, New York